

Argonne National Laboratory

A HEAT-PIPE-COOLED FAST-REACTOR SPACE POWER SUPPLY

by

J. J. Roberts, E. J. Croke,
R. P. Carter, and J. E. Norco

The facilities of Argonne National Laboratory are owned by the United States Government. Under the terms of a contract (W-31-109-Eng-38) between the U. S. Atomic Energy Commission, Argonne Universities Association and The University of Chicago, the University employs the staff and operates the Laboratory in accordance with policies and programs formulated, approved and reviewed by the Association.

MEMBERS OF ARGONNE UNIVERSITIES ASSOCIATION

The University of Arizona
Carnegie-Mellon University
Case Western Reserve University
The University of Chicago
University of Cincinnati
Illinois Institute of Technology
University of Illinois
Indiana University
Iowa State University
The University of Iowa

Kansas State University
The University of Kansas
Loyola University
Marquette University
Michigan State University
The University of Michigan
University of Minnesota
University of Missouri
Northwestern University
University of Notre Dame

The Ohio State University
Ohio University
The Pennsylvania State University
Purdue University
Saint Louis University
Southern Illinois University
University of Texas
Washington University
Wayne State University
The University of Wisconsin

LEGAL NOTICE

This report was prepared as an account of Government sponsored work. Neither the United States, nor the Commission, nor any person acting on behalf of the Commission:

A. Makes any warranty or representation, expressed or implied, with respect to the accuracy, completeness, or usefulness of the information contained in this report, or that the use of any information, apparatus, method, or process disclosed in this report may not infringe privately owned rights; or

B. Assumes any liabilities with respect to the use of, or for damages resulting from the use of any information, apparatus, method, or process disclosed in this report.

As used in the above, "person acting on behalf of the Commission" includes any employee or contractor of the Commission, or employee of such contractor, to the extent that such employee or contractor of the Commission, or employee of such contractor prepares, disseminates, or provides access to, any information pursuant to his employment or contract with the Commission, or his employment with such contractor.

Printed in the United States of America
Available from

Clearinghouse for Federal Scientific and Technical Information
National Bureau of Standards, U. S. Department of Commerce
Springfield, Virginia 22151

Price: Printed Copy \$3.00; Microfiche \$0.65

ANL-7422

Propulsion Systems and

Energy Conversion (TID-4500)

AEC Research and

Development Report

ARGONNE NATIONAL LABORATORY

9700 South Cass Avenue

Argonne, Illinois 60439

A HEAT-PIPE-COOLED FAST-REACTOR
SPACE POWER SUPPLY

by

J. J. Roberts, E. J. Croke,
R. P. Carter, and J. E. Norco

Reactor Engineering Division

June 1968

TABLE OF CONTENTS

	<u>Page</u>
ABSTRACT	5
I. INTRODUCTION	5
II. REACTOR DESIGN SUMMARY	7
III. CRITICALITY STUDIES AND NUCLEAR-MATERIALS SELECTION	17
A. Criticality Studies	17
B. Nuclear Materials Survey	17
1. Fuel Survey	17
2. PuP Characteristics	19
3. Reflector Materials	19
IV. HEAT-TRANSFER STUDIES	20
A. General	20
B. Primary Heat-pipe Design	21
C. Heat-pipe Radiator	25
V. REACTOR OPTIMIZATION	28
VI. RADIAL REFLECTOR	29
VII. NUCLEAR SHIELDING	30
VIII. CONTROL	31
A. Reactivity Coefficients	31
B. Startup	32
IX. CONCLUSIONS	33
ACKNOWLEDGMENT	33
REFERENCES	34

LIST OF FIGURES

<u>No.</u>	<u>Title</u>	<u>Page</u>
1.	Fast-reactor Space Power Supply	7
2.	Sectional View of Fast-reactor Space Power Supply	8
3.	Heat-transfer Components	10
4.	Core Containment Vessel with Heat Pipes and High-temperature Shell Installed	11
5.	Fuel-element Alignment and Support System	11
6.	Cutaway View of Control Module	13
7.	Core Radial Power Profile	23
8.	Fuel-element Peak Temperatures vs Power	24
9.	Core Axial Temperature Distribution	24
10.	Core Radial Temperature Distribution	24
11.	Frequency of Meteor Penetrations	25
12.	Figure of Merit for Heat-pipe Fluid	27
13.	Core Parameters vs Fuel-element Size	29
14.	Dose Rate vs Reflector Thickness	29
15.	Core-edge Power Peak vs Reflector Thickness	30
16.	Core Mass vs Reflector Thickness	30
17.	Reactivity vs Reflector Thickness	32

LIST OF TABLES

<u>No.</u>	<u>Title</u>	<u>Page</u>
I.	Compact Reactor Parameters	14
II.	Fuel Properties	17
III.	Reflector Properties	20

A HEAT-PIPE-COOLED FAST-REACTOR SPACE POWER SUPPLY

by

J. J. Roberts, E. J. Croke,
R. P. Carter, and J. E. Norco

ABSTRACT

A fast-spectrum, nuclear-reactor power supply was designed which compares favorably with radioactive isotope sources and SNAP thermal reactors in the 1-5-kWe range. The use of a ^{239}Pu -based fuel in a relatively simple design, which employs in-core heat pipes and a heat-pipe radiator, yields a comparatively lightweight and low-cost system, which should have good intrinsic reliability.

The specific weight for the proposed 1-kWe reactor system is about 525 lb/kWe (340 lb/kWe at 5 kWe), as compared to typical weights of about 1000 lb/kWe for isotope powered supplies and more than 800 lb/kWe for existing SNAP thermal-reactor designs in this power range. Unlike competitive isotopes, ^{239}Pu (a by-product of the continuously expanding, light-water reactor industry) will be available to meet the anticipated demand for unmanned experimental communication satellites in the 1970's. Moreover, the production cost of this fuel should be approximately 20-70% of the equivalent in isotope power in the 25-125-kWt thermal-power range.

I. INTRODUCTION

As opportunities for launching satellites and probes become increasingly available to military, scientific, and commercial users, the demand for low-power electrical supplies in the 1-10-kWe range¹ will increase. Projected requirements for manned space laboratories also fall within this power range.² Ideally, these demands should be met by a single system, which can be integrated into this complex of foreseeable missions.

Recent developments in thermoelectric and thermionic devices have given static converters a special appeal for use in space power systems. Feasibility testing of thermoelements having a hot-junction temperature as high as 1200°C has been performed.³ This upward trend of thermocouple

temperatures permits higher radiator temperatures, lower system specific weights, and greater radiation stability of thermoelectric materials than have hitherto been considered for space power systems.⁴ On the other hand, the minimum practical emitter temperature for thermionic diodes has dropped to around 1200°C,⁵ closer to the maximum source temperatures of present designs of nuclear reactors and isotopic energy supplies. The state of the art of thermoelectric converter design is slightly more advanced in the 1200°C range than for thermionic generators, but the availability of a reliable high-temperature source will spur the development of thermionic devices with probable efficiencies of 15%,⁵ as opposed to 4% for thermoelectric converters.³ To date, thermionic modules have been tested with efficiencies from 6% at an emitter temperature of 1200°C⁶ to 11% at 1350°C. Power densities of 2 W/cm² have been demonstrated.^{7,8}

To attain high system efficiency and/or attractive specific weights, it is reasonable to assume that the search for an all-purpose 1-10-kWe power supply will focus on source temperatures of at least 1200°C. This report outlines the design parameters of a compact, fast-reactor power supply which will satisfy this need. The concept is based on a relatively simple combination of a new high-temperature fuel, plutonium monophosphide, and the newest development in heat-transfer technology, the ubiquitous heat pipe.

Since the converter elements can be supplied with up to 100 kWt at 1350°C, this system can be coupled with highly efficient thermionic diodes to produce up to 10 kWe. The specific weights are quite attractive: 525 lb/kWe at 1 kWe and 340 lb/kWe at 5 kWe for the 4% efficient thermoelectric version discussed in Section II of this report. With an 11% efficient thermionic converter, the system would yield specific weights of 100 lb/kWe at 5 kWe and 73 lb/kWe at 10 kWe. These figures may be compared to unshielded weight estimates for SNAP-8 systems of 633 lb/kWe at 1 kWe and 290 lb/kWe at 20 kWe.¹ Since the SNAP-8 lithium hydride moderator has a vapor pressure of 5 atm at 1100°C,⁹ its use with a thermionic system does not appear feasible unless a two-zone core design can be developed in which high temperatures can be tolerated.

The fissionable constituent of the reactor fuel is ²³⁹Pu. This by-product of the continuously expanding light-water reactor industry will be available to meet the anticipated demand for unmanned satellites in the early 1970's.¹⁰ Moreover, a reasonably firm production-cost prediction of \$10/g (Ref. 11) implies a fuel inventory of about \$380,000 per reactor, a figure that is essentially independent of the thermal-power level.

II. REACTOR DESIGN SUMMARY

The reference design for the compact reactor was configured as a 1-kWe space power supply using a thermoelectric generator operating between a hot-junction temperature of 1200°C and a cold-junction temperature of 510°C.

The reactor core (shown in Figs. 1 and 2) consists of an aggregate of 36 unclad fuel elements, each a hexagon 2.6 cm across the flats and 27 cm long. The fuel is plutonium monophosphide, a novel compound synthesized first by O. Kruger and J. Moser of Argonne National Laboratory.¹² This material has thermodynamic, chemical, and physical properties which, on the basis of sample testing, appear to be superior to the more popular PuO_2 and PuC .

The fuel elements are positioned by, but not bonded to, 36 heat pipes, which pierce one end of the molybdenum core-containment vessel. These 7/16-in.-OD molybdenum pipes contain a composite grooved-channel and screen-mesh molybdenum wick and use lithium as the working fluid. The central position in what is basically a 37-fuel-element array is left void to simplify the routing of the heat pipes (as shown in Fig. 2).

After core assembly, the containment vessel is purged and welded gas-tight under 1 atm of helium. Heat transfer from the fuel across a 2-mil gap to the lithium heat pipe is by radiation and conduction through the helium; however, conduction is the dominant mode. The maximum temperature attained by the fuel is 1269°C, well below the melting or dissociation limits for PuP .¹³

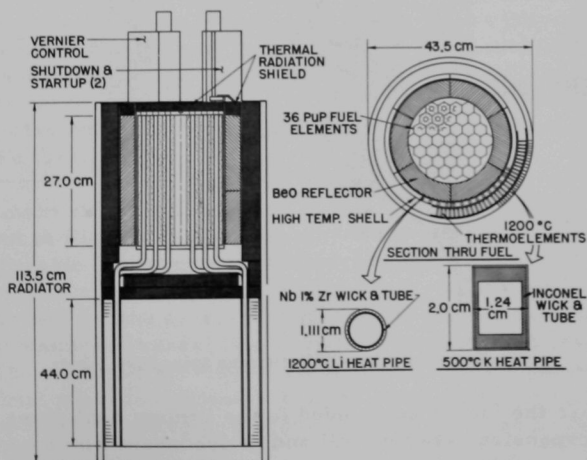


Fig. 1. Fast-reactor Space Power Supply

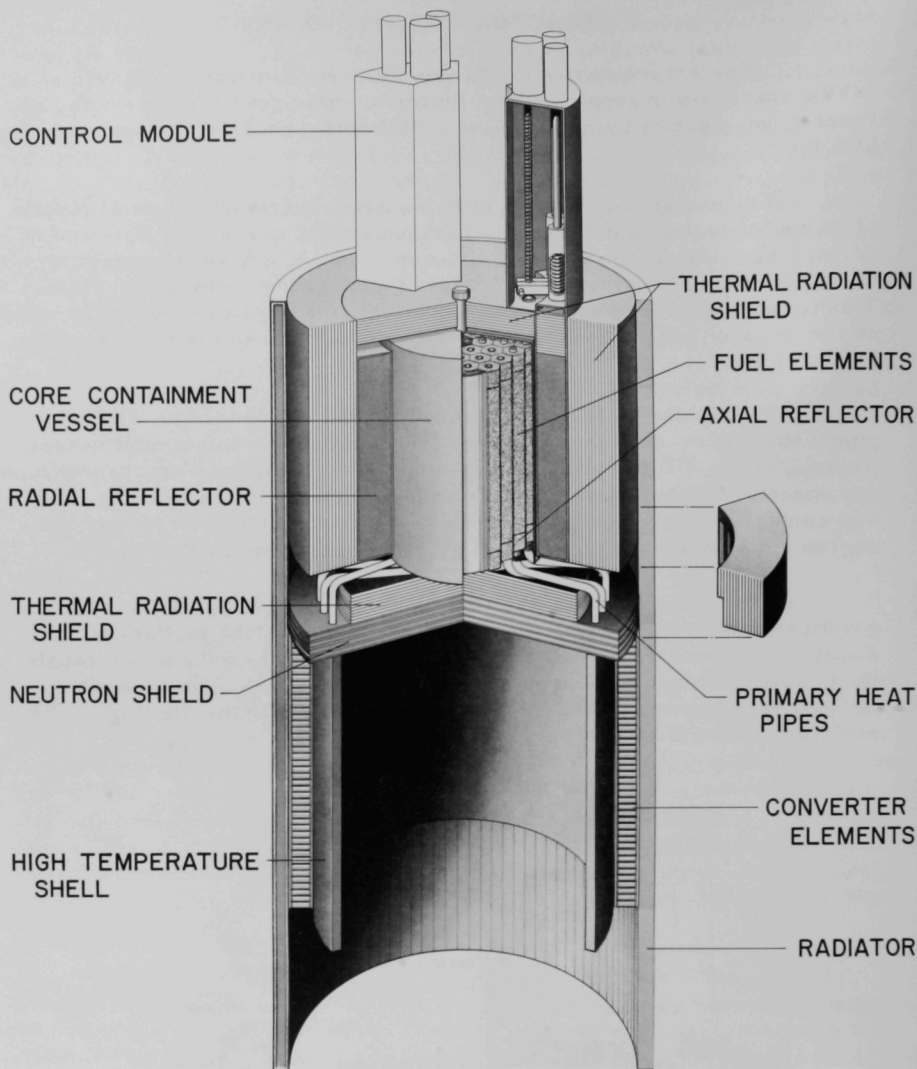


Fig. 2. Sectional View of Fast-reactor Space Power Supply

Because the fuel is not bonded to the lithium heat pipes, the differential thermal expansion between PuP and molybdenum which occurs during startup poses no problem. Since each heat pipe emerges from the containment vessel through a moderately flexible, welded molybdenum bellows,

differential expansion of the heat pipes and the vessel is accommodated without imposing excessive thermal stresses on the heat pipes or compromising the gas-tight integrity of the vessel.

Between the core (evaporator) and the hot shell (condenser), each heat pipe undergoes two 90° bends (as shown in Fig. 3). In this transition section, radiation-heat losses are minimized by a 4.0-cm, multilayer, axial thermal-radiation shield which reduces the net axial radiation-heat loss to approximately 2% of the core thermal power. A similar axial shield suppresses radiation-heat losses from the opposite end of the core.

A 5-cm-thick radial reflector of beryllium oxide serves as a radiation shield for the thermoelements and permits the required fuel loading for a bare core to be reduced from about 60 to 38 kg. This core-reflector combination is near optimum from a weight standpoint. The reflector also flattens the core radial power profile and thereby tends to equalize the thermal load on the heat pipes. For fuel economy, 3-cm-long BeO axial reflector pieces, similar in design to the PuP elements, were added, top and bottom, within the core container (as shown in Fig. 3).

The hot shell is a 33.4-cm-dia, 44-cm-long cylinder, formed by molybdenum webs between the condenser sections of the 36 molybdenum heat pipes. For the thermoelectric version of the system, 2222 3/8-in-dia thermocouples, typical of the high-temperature (1200°C) devices developed for the Air Force by Monsanto Chemical Corporation,³ are mounted on the exterior surface of this shell. The same shell would serve as the emitter heat source for a thermionic generator.

Heat is rejected to space at 500°C through a radiator assembly composed of 100 rectangular-cross-section, double-ended potassium heat pipes. The radiator assembly is fabricated from 20-mil Inconel tubing and takes the form of a 43-cm-OD, 113-cm-long, cylindrical shell (as shown in Fig. 1). With a 5-kWe thermionic converter having a collector temperature of 600°C, the radiator size and weight are approximately the same as those required for the 1-kWe thermoelectric system.

The main structural member of the system is the core containment vessel (shown in Fig. 4). Six equidistant radial ribs, which protrude from the vessel, provide mounting and structural support for the reflector segments and for the six segments of the hot shell. These ribs also provide attachment points for the axial thermal shields and the radiator shell. Within the containment vessel is a hexagonal molybdenum insert, which fits around the core and provides for the support and alignment of the lower ends of the heat pipes (as shown in Fig. 5). Radial shielding, which minimizes the thermal radiative heat transfer from the core to the reflector, is mounted on this insert.

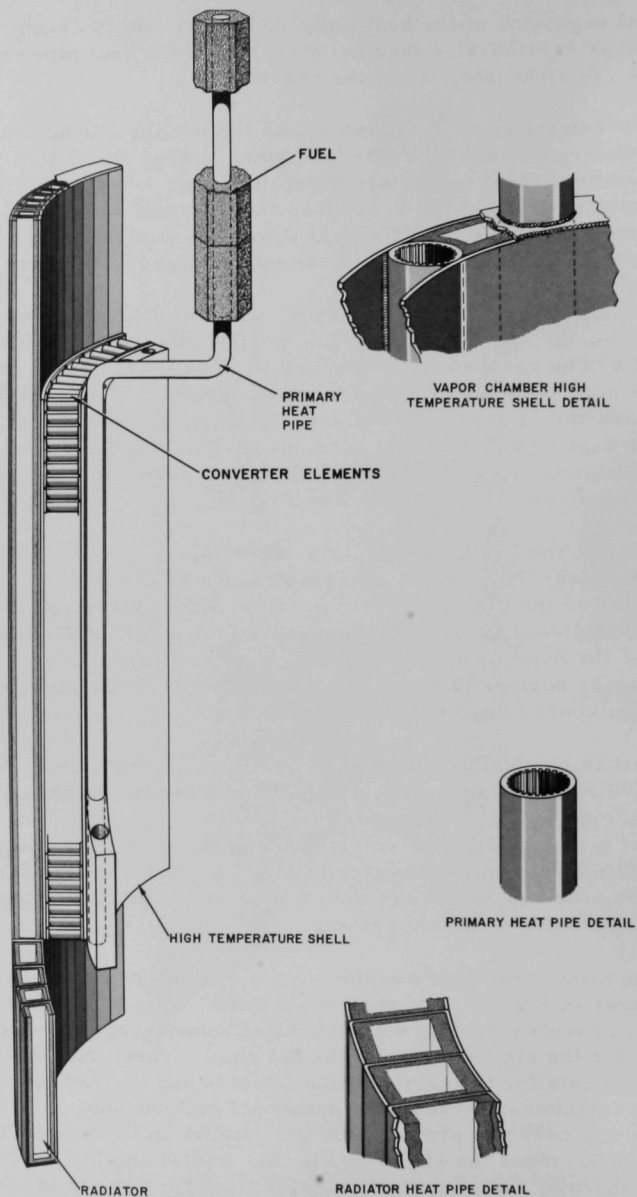


Fig. 3. Heat-transfer Components

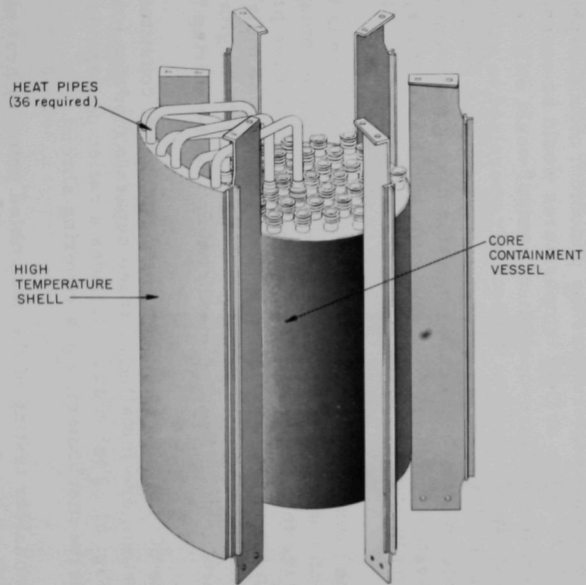


Fig. 4. Core Containment Vessel with Heat Pipes and High-temperature Shell Installed

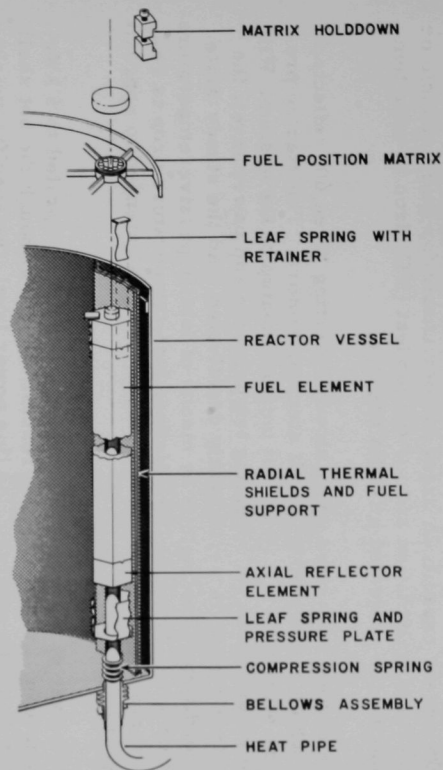


Fig. 5. Fuel-element Alignment and Support System

The thermal power of the reactor is 27.6 kWt, and its design life is 10,000 hr. The power-conversion system efficiency of the reference thermoelectric generator was assumed to be 4%. The system was sized to provide 10% excess capacity in order to compensate for thermocouple or thermionic-diode malfunction and for the modest (6°C) drop in core temperature during the projected mission lifetime.

The system is started up by slowly inserting three 60° reflector segments, which are driven by small stepping motors. The startup program occurs slowly enough to permit uniform heatup of the system. With the system stabilized at its operating temperature and power level, the startup control system is permanently deactivated, and the steady-state operating condition is maintained by means of totally passive temperature-coefficient control. Since an 18°C lifetime fuel-temperature drop is regarded as tolerable, the effective mission life can be extended to approximately 3 years.

The power of the thermoelectric system can be uprated to 5 kW_e without significant alteration of the reactor design, although the hot shell and radiator would be enlarged. At this power level, the specific weight of the system would be reduced to about 340 lb/kW_e. The maximum fuel temperature associated with a 5-kW_e output would be 1590°C, still within the range of stable performance for plutonium monophosphide under 1 atm of helium.¹³⁻¹⁵ Other system temperatures would be essentially unchanged, and passive, temperature-coefficient control would still be feasible. The lithium heat pipes have been deliberately oversized to accommodate this higher power. If the same core-reflector-heat pipe-radiator combination were coupled with a thermionic generator having a system efficiency of 11%, the system would produce approximately 5 kW_e at a specific weight of about 100 lb/kW_e.

The mechanical design of the reactor system lends itself to ease of assembly and handling. The core is assembled in the containment vessel by sliding the fuel pieces over the heat pipes, which have previously been inserted in the vessel and welded to the flanges on the molybdenum heat-pipe bellows. The heat pipes can accommodate both longitudinal and lateral displacements due to thermal expansion during the startup transient.

The 60° movable reflector segments, which constitute the startup control system, are installed as three separate modules (one of which is shown in Fig. 6). Each module includes a reflector segment, a stepping motor, a drive mechanism, and a covering shroud.

Nonnuclear testing of the assembled primary heat pipe, power converter, and radiator is quite feasible for this system. The design lends itself to electrical heating of the primary heat pipes, since the entire system

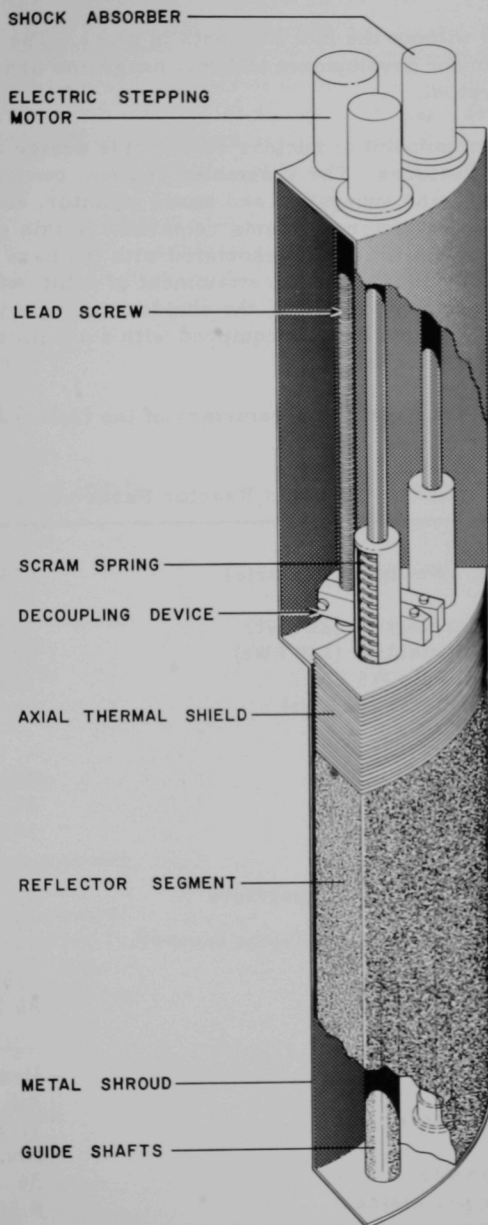


Fig. 6. Cutaway View of Control Module

can be assembled without the fuel elements in place. The nuclear and nonnuclear component development and test programs are thus quite separable for this system.

From the standpoint of nuclear safety, this design concept includes several desirable features. The assembled system, complete with electrical power-conversion subsystem and space radiator, can be shipped and handled with all the reflector segments removed. In this condition, a 20% shutdown safety margin ($\Delta k/k$) is associated with the bare core. During prelaunch operations and before the attainment of orbit, with the three stationary reflector segments in place, the shutdown margin is 6%. Each of the movable reflector segments is equipped with a scram spring, which is restrained by a magnetic latch.

Table I lists the various parameters of the fast-reactor space power supply system.

TABLE I. Compact Reactor Parameters

<u>System Performance</u>	
Total weight (1 kWe thermoelectric)	525 lb
Specific weight	
1 kWe thermoelectric (25 kWt)	525 lb/kWe
5 kWe thermoelectric (125 kWt)	340 lb/kWe
5 kWe thermionic (46 kWt)	100 lb/kWe
10 kWe thermionic (92 kWt)	73 lb/kWe
<u>Core</u>	
Type	Fast, reflected
Active length	27 cm
Critical diameter	16.6 cm
<u>Plutonium Monophosphide Fuel</u>	
Fuel density at operating temperature	8.41 g/cc
Fuel, v/o in core	67.5
Reference thermal power	27.5 kWt
Peak fuel temperature	1269°C
Fuel weight	86 lb
<u>Fuel Elements</u>	
Configuration	Hexagonal
Across flats	2.6 cm
Central hole diameter	1.12 cm
Cladding	None
Number of elements	36
Average power per element	0.764 kWt
Limiting temperature capability at 1 atm helium	1700°C

TABLE I (Contd.)

Radial Reflector

Material	Beryllium oxide
Density at operating temperature	2.6 g/cc
Melting point	2550°C
Cylindrical OD	29.9 cm
Length	30 cm
Thickness	5 cm
Weight	66 lb

Axial Reflector

Material	Beryllium oxide
Segment length	3.0 cm

Primary Heat Pipes

Material	Molybdenum
Evaporator length	27 cm
Transition section length	23 cm
Condenser length	44 cm
Outside diameter	1.11 cm
Wall thickness	0.101 cm (40 mils)
Channel wick	
Number of channels	51
Channel width	0.204 mm
Channel depth	0.510 mm
Screen wick	
Thickness	0.22 mm
Porosity	0.5
Permeability	12
Pore radius	0.08 mm
Working fluid	Lithium
Reference design power	0.88 kWt
Operating pressure	5.3 psia
Operating temperature	1200°C
Vapor pressure drop (reference power)	0.0235 psid
Liquid pressure drop	0.1544 psid
Vapor temperature drop	0.655°C

Radiator Heat Pipes

Material	Inconel
Total length	113.5 cm
Evaporator length	44 cm
Condenser length	113.5 cm
Width	1.35 cm
Height	2.0 cm
Wall thickness	0.051 cm (20 mils)

TABLE I (Contd.)

<u>Screen wick</u>	
Inner- and outer-wick thickness	0.314 cm
Lateral-wick thickness	0.1517 cm
Porosity	0.5
Permeability	12
Pore radius	0.025 cm
Working fluid	Potassium
Reference design power per pipe	0.264 kWt
Operating pressure	0.5 psia
Operating temperature	500°C
Vapor-pressure drop	0.005 psia
Liquid-pressure drop	0.005 psia
Vapor-temperature drop	2.93°C
Total wall-temperature drop	11.9°C
<u>Hot Shell</u>	
Material	Molybdenum
Operating temperature	1200°C
Thickness	1.3 cm
Outside diameter	33.5 cm
Length	44 cm
<u>Core Containment Vessel</u>	
Material	Molybdenum
Outside diameter (cylindrical)	30.3 cm
Length	32.8 cm
Radial wall thickness	0.25 cm
End-cap thickness	0.5 cm
<u>Axial Thermal-radiation Shields</u>	
Material	Molybdenum
Lamina thickness	0.020 in.
Number of laminae	15
Total thickness	3.95 cm
Diameter	37.50 cm
Temperature of radiating surface	500°C
<u>Thermoelectric Generator</u>	
Hot-junction temperature	1200°C
Cold-junction temperature	510°C
Number of thermocouple pairs	2222
Power per couple	0.495 W
Total power (reference thermoelectric)	1 kW _e
Voltage (reference)	40 V

III. CRITICALITY STUDIES AND NUCLEAR-MATERIALS SELECTION

A. Criticality Studies

The reactor criticality calculations required during this study were performed with the SNARG-1D multigroup Sn code using the S4 option. Higher-order approximations yield negligible improvements in estimations of critical masses or multiplication constants. Multigroup diffusion theory does not apply since the core radius is less than five mean free paths. Hanson and Roach¹⁶ 16-group cross sections were obtained from ANL Set 201, augmented to include ³¹P.

B. Nuclear Materials Survey

1. Fuel Survey

The nuclear criteria for the compact reactor are similar to those proposed by MacFarlane⁹ and others for low-power conduction-cooled systems. The compact reactor should be a fast assembly, reflected, if at all, for purposes of power flattening and/or for neutron shielding. MacFarlane⁹ has shown that, although some moderated systems have lower critical masses than those that use pure fuel, the low melting points of most lightweight diluents are an overriding disadvantage.

The objective of this section is to identify suitable core materials and then select the most promising fuel for the design of the reference system. Table II represents a survey of potential fuels. Because projected

TABLE II. Fuel Properties

Fuel	Theoretical Density, g/cc	Melting Point, °C	Thermal Conductivity, W/cm·°C	Bare Sphere Critical Radius, cm	Bare Sphere Critical Mass, kg	References
²³⁵ U	18.8	1132	0.536 at 900°C	8.4	46	6
²³³ U	18.8	1132	0.536 at 900°C	5.8	10	6
²³⁹ Pu	19.7	680	0.209 at 600°C	5.0 ^a	10	6
²³⁵ U	12.3	2400	0.251	11.8	84	6
²³⁵ UO ₂	10.0	2750	0.025 at 900°C	14.2	120	6, 17
²³⁵ UO ₂ --20 v/o Mo	10.1	-	0.24 at 870°C	16.2 ^b	168	15
²³³ U	12.3	2400	0.251	8.4	31	6
²³³ UO ₂	10.0	2750	0.025 at 900°C	10	42	6
²³³ UO ₂ --20 v/o Mo	10.01	-	0.24 at 870°C	11.5	64	15
²³⁹ PuC	13.6	1654	0.1 at 400°C	7.6 ^c	22	6, 19, 20
²³⁹ PuO ₂	10.0	2400	0.025 at 900°C	9.3	34	6
²³⁹ PuC--20 v/o ZrC	11.12	~2000	-	8.9	33	6
²³⁹ PuO ₂ --20 v/o Mo	9.69	<2000	0.23 at 900°C	10.8	51	15
²³⁹ PuP	9.89	2600	0.09	10.3	45	9, 16

^a96% enrichment.

^b94% theoretical density.

^c90% theoretical density.

converters operate at 1200-1350°C, the fuel must be stable up to at least 1500°C and higher for uprated versions. This criterion eliminates the pure metals and renders PuC only marginally acceptable. Table II shows that ^{235}U systems would be significantly larger (but probably more economical) than those with plutonium-based fuels. In view of this fact, and because compactness is a first-order design goal, all ^{235}U compounds were eliminated as candidate fuels.

As expected, ^{233}U and ^{239}Pu compounds yield very compact systems, and, as shown in Table II, several fuels based upon these fissile materials have such desirable properties as high melting point and high thermal conductivity. Especially promising are ^{233}UC and the $^{233}\text{UO}_2$ --20 v/o Mo cermet if UC can be made available in sufficient quantities. Although there is at present no systematic production of ^{233}U via a thorium fuel cycle, it has been estimated that the isotope production reactors at Hanford, Washington, can produce an adequate supply.⁹

One attribute of ^{233}U that weighs greatly in its favor when it is compared to ^{239}Pu -based fuels is its relatively low toxicity. For example, the maximum permissible airborne concentration of ^{233}U is $2 \times 10^{-9} \mu\text{g}/\text{ml}$, as opposed to $3 \times 10^{-11} \mu\text{g}/\text{ml}$ for ^{239}Pu . This comparison is especially impressive when it is extended to include radioactive isotope fuels such as ^{210}Po ($4 \times 10^{-14} \mu\text{g}/\text{ml}$) and ^{90}Sr ($1 \times 10^{-12} \mu\text{g}/\text{ml}$).¹⁷

Despite the advantages of ^{233}U compounds, the ^{239}Pu fuels were favored in this preliminary design because of the availability of this isotope as a by-product of the continuously expanding, light-water reactor industry and the future fast-breeder-reactor program. Among the plutonium compounds, PuC is undesirable because of its relatively low melting point and poor compatibility with most structural materials above 1300°C.¹⁸ Although plutonium dioxide has a low thermal conductivity, the maximum fuel temperature (approximately 1500°C) at the outer surface of a PuO_2 fuel element would be considerably below the melting point of the fuel. However, the reactor design could not be uprated to 5-10 kWe because the PuO_2 fuel temperatures and resultant dissociation pressures associated with higher power operation would be excessive.¹⁹ The PuC-ZrC system was listed because studies with uranium carbide show that the melting point of UC increases almost linearly when ZrC is added to form a solid solution. A similar effect might be predicted for PuC-ZrC, but since this analogous mixture has not been prepared,²⁰ it would not be an appropriate choice for this design. Similarly, the $^{239}\text{PuO}_2$ --20 v/o Mo cermet would represent an improvement on the thermal conductivity and stability of plutonium dioxide,²¹ but published data are not available for this material.

There are at least three remaining candidates among the plutonium compounds: PuN, PuS and PuP. Plutonium mononitride has received much attention; for example, a 1965 Nucleonics article rated it the most

promising fast-reactor fuel.²² However, this material will probably be inferior to the monophosphide because of its high vapor pressure at elevated temperatures.^{13,22} Plutonium monosulphide and monophosphide are similar in physical properties, but the former is comparatively difficult to produce in stoichiometric composition.¹² Therefore, from among the potentially suitable fuels, plutonium monophosphide is chosen as the reference fuel.

2. PuP Characteristics

Plutonium monophosphide is a dark-grey, metallic-appearing ceramic, which appears to have very attractive physical properties at elevated temperatures. Kruger and Moser¹² have prepared high-purity, 40-g samples of the compound by reaction of the metal hydride with the phosphide. Since the monophosphide is the only stable high-temperature compound in the PuP system, the stoichiometric composition is easily obtained. This method of preparation is quite suitable for large-scale production using fluidized-bed techniques.

Observations of the compound made during sintering indicated that it is stable¹³ up to 1500°C in vacuum and 1700°C under 1 atm of argon, and the vaporization and dissociation rates are negligible. Melting and rapid decomposition occur at 2600°C.¹² The linear-expansion coefficient, $11.9 \times 10^{-6}/^{\circ}\text{C}$,²³ and the thermal conductivity, $0.09 \text{ W/cm}^{\circ}\text{C}$,¹³ were found to be nearly invariant with temperature.

The low fuel burnup ($<0.05\%$) that characterizes the compact reactor, coupled with the absence of corrosion or erosion mechanisms typical of liquid-metal-cooled reactors, and the excellent stability of the fuel permit the PuP fuel elements to be unclad. In addition, since helium is used as the thermal coupling between fuel element and heat pipe, the material-development problems normally associated with high-temperature bonding are avoided. The compatibility, at high temperatures, of PuP and the primary heat-pipe structural material, molybdenum, represents a second-order material problem, which must be investigated. These characteristics make possible a relatively simple design and serve to facilitate the fabrication, assembly, and testing of the system, as described in Section II.

3. Reflector Materials

Table III is a partial listing of the reflector materials considered for the compact fast reactor. Beryllium oxide (with graphite running a close second) best satisfies the major requirements of a high melting point, a low dissociation rate, a low density, and good neutron-scattering properties. Beryllium carbide was eliminated because its dissociation rate is equivalent to $1 \times 10^{-3} \text{ g/sec-cm}^2$ at 1200°C, while that of BeO is

only 3×10^{-13} g/sec-in.² (Ref. 24). The latter figure implies a loss of only 0.6 g over the 10,000-hr mission life of the reactor.

TABLE III. Reflector Properties

Material	Theoretical Density, g/cc	Melting Point, °C	Reflector Savings for PuC Sphere with 4-cm Reflector, cm	Mass of 4-cm Reflector, kg	References
C	1.6	Sublimes $P_{\text{atm}} = 10^{-14}$ at 1300°C	1.03	6.0	17, 18
Be	1.85	1284	1.83	5.7	6, 18
Be ₂ C	2.4	Dissociates $P_{\text{atm}} = 4 \times 10^{-4}$ at 1300°C	2.01	7.1	17
BeO	3.025	2550	2.02	8.9	17, 18
LiH		688			6
ZrH ₂		1093			6
Ni	8.9	1455	1.29	31.4	18
Fe	7.86	1539	1.06	29.2	18

Graphite, with a thermal conductivity as high as 0.6 W/cm-°C,²⁴ might be preferred over BeO (0.2 W/cm-°C) for a purely conduction-cooled reactor design,³ but this advantage is unimportant for a system in which the primary heat-transfer path is provided by heat pipes.

IV. HEAT-TRANSFER STUDIES

A. General

The use of heat pipes in the core and for the space radiator was an obvious choice for a system intended to bridge the gap between the simple, but low-power (0.3-0.5 kW), conduction-cooled, nuclear-thermoelectric generator such as those proposed by MacFarlane⁹ or Monsanto Corporation,³ and the more complicated, higher-power (0.5-350 kW), liquid-metal-cooled space-power thermoelectric or turboelectric systems, such as SNAP-10A or SNAP-50. The heat pipe offers the prospect of extracting and rejecting significant amounts of power from a reactor system without the compromise of reliability or operating life that is associated with multiloop, liquid-metal coolant systems that use high-temperature rotating machinery. Moreover, a heat-pipe radiator can be constructed in a totally modular fashion to minimize the meteor damage hazard that is present with conventional liquid-metal radiators, or even with vapor-chamber fin radiators such as those proposed by Haller and Lieblein.²⁵

B. Primary Heat-pipe Design

The 36 circular, in-core primary heat pipes are identical in cross section and heat-transfer capacity and were sized to accommodate the peak power (0.88 kW) generated in each of the six members of the inner ring of fuel elements.

The operating temperature of the primary heat pipes corresponds to a 1200°C thermoelement hot junction or 1350°C thermionic temperature. In this temperature range, lithium represented the optimum choice for the heat-pipe fluid. This selection was governed by a number of considerations:

1. At temperatures in excess of about 900°C, above which the vapor pressure of lithium is sufficiently high to permit efficient heat-pipe operation, the high surface tension and low liquid density of lithium render it an excellent fluid for use in a "capillary pump."
2. Since lithium has a relatively low vapor pressure (5 psi at 1200°C and 20 psi at 1350°C), it does not need to be contained within a thick-walled pipe structure; thus, both weight and temperature drop across the heat-pipe walls can be minimized with a lithium system.
3. The high latent heat of vaporization of lithium yields the maximum cross-sectional heat flux for a given heat-pipe diameter, and, if the lithium pipe is somewhat oversized, potential startup problems can be minimized.
4. The extremely large heat-transfer capacity of a lithium pipe lends itself to the design of a system that can be uprated to higher power levels with minimal modification of the primary heat-pipe configuration.

From the limited number of refractory metals compatible with lithium at 1200°C (niobium, tantalum, molybdenum, and their alloys), molybdenum was chosen for the heat pipe and wick. Nb-1% Zr would have been acceptable on the basis of the results of Li-Nb--1%-Zr heat-pipe tests reported²⁶ by the Los Alamos Scientific Laboratory (LASL). These tests verified the compatibility of the lithium-niobium combination at temperatures in excess of 1100°C for operating duration up to 3500 hr, including a number of restart cycles. Romano, Fleitman, and Klamut found that lithium and niobium are compatible at temperatures as high as 1150°C for up to 6500 hr,²⁷ and the LASL test series included runs at temperatures as high as 1300°C; however, experimental verification of 10,000-hr compatibility remains to be established. Although Nb-1% Zr appears to be appropriate for 1200°C operation, the prospect of operating the system at 1350°C with a thermionic converter indicated the desirability of fabricating the primary heat pipes of tungsten-zirconium-molybdenum (TZM). The compatibility of lithium and TZM for long-duration heat-pipe operation was established in tests conducted by RCA⁸ at temperatures up to 1500°C.

The sizing of the heat pipes was dictated by the following considerations:

1. The heat-pipe wick and vapor-passage cross sections must be adequate to carry the required design power.
2. The heat flux across the pipe surface must be low enough to preclude boiling in the wick.
3. The pipe diameter must be large enough to maintain the fuel-element temperature below its 1700°C limit.
4. The pipe diameter must be large enough to ensure a near-uniform temperature distribution on the cylindrical shell that is in contact with the thermocouple hot junctions.
5. The heat pipes should be sufficiently large so that the system can be uprated from its design thermal-power level of 25 kWt to at least 125 kWt without significant modification of the reactor design.

The lithium heat-pipe wick is configured as a combined grooved-channel and screen-mesh design. The grooved-channel approach, in which the wick consists of an array of rectangular channels milled into the inner surface of the pipe wall, has the significant advantage that the wick cannot, under any circumstances, separate from the wall and produce hot spots. The grooved-channel wick also lends itself to analysis more readily than does the screen-mesh wick, since the flow characteristics (flow area, hydraulic diameter, etc.) of the grooved-channel wick can be characterized more accurately than those of the screen-mesh wick. An open-channel wick does, however, suffer the disadvantage that the capillary forces associated with it are approximately half those of a screen-mesh wick, since the radius of curvature of the liquid meniscus for the grooved channel is effectively infinite in the axial direction. The open channel is, moreover, sensitive to a start-transient problem in that, at low temperatures, an interaction between the high-velocity vapor and the liquid surface tends to retard the flow of the liquid and prevent startup.²⁸

Although its performance characteristics are more difficult to define, the screen-mesh wick is superior to the grooved-channel type as a capillary pump and is relatively insensitive to the start-transient, vapor-liquid interaction. The tendency of the screen to detach itself from the walls of the heat pipe represents the major disadvantage of this type of wick.

The primary heat pipes of the compact reactor combine the features of both types of wick. Fifty-one rectangular channels, having a depth of 0.510 mm and a width of 0.204 mm (shape factor of 1.5), are equally spaced around the inner surface of the 1.01-mm (40-mil)-thick walls of the heat pipe.

The effective channel capillary-pore radius of 0.102 mm is sufficient to wick the liquid lithium to a height of 45 cm against the equivalent of one gravity. This wicking height corresponds to the length of the evaporator leg of the heat pipe; thus, the core-primary heat-pipe subassembly can function in earth-normal gravity for ground-testing of the space system and can, moreover, be readily adapted for terrestrial or undersea use.

The channels are sized to carry the full 0.88-kW heat load of the high-temperature central elements; however, additional capacity is provided by a single layer of molybdenum screen in close contact with the inner surface of the pipe. This 0.22-mm-thick screen has an equivalent pore radius of 0.08 mm, a permeability of 12, and a void fraction of 0.5. It is included primarily to facilitate the startup of the system since it will serve as a barrier between the vapor and the liquid during the low-temperature portion of the start transient, however, it also adds the equivalent of about 150 W of heat-transfer capacity to the reference pipe.

Because of the excellent thermal properties of lithium, the first two criteria noted previously for heat-pipe sizing were not important at the design power level. Neither did the third criterion prove to be significant for the fuel-element configuration, since the highest temperature attained by any fuel element (i.e., that associated with a central element at the core midplane) did not exceed 1269°C at the design power level. Figure 7 shows the radial power distribution of the system in terms of the neutron-flux distribution. The limiting temperature (1700°C) for these 2.6-cm across-

flats hexagonal elements is reached at a thermoelectric power level of 7.2 kWe. Figure 8 shows the variation of peak fuel temperature with power for several different fuel-element sizes. Figures 9 and 10 show the axial and radial temperature variation in the core at the reference power level.

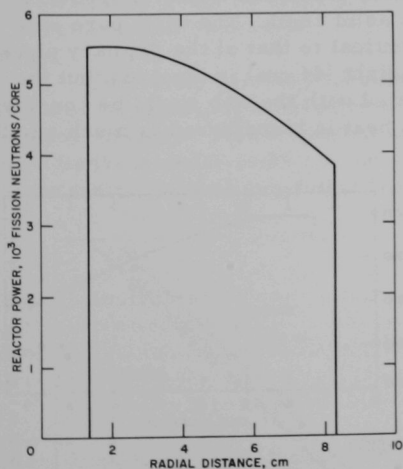
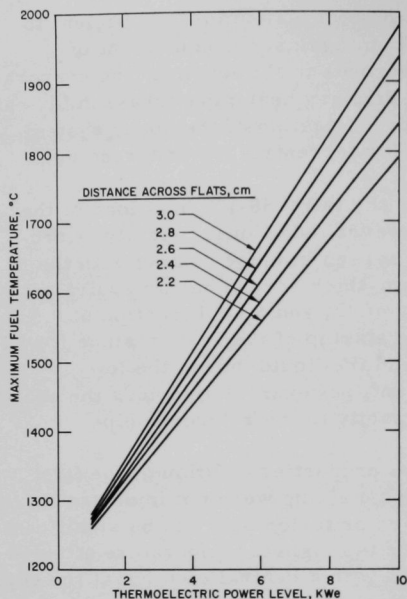


Fig. 7. Core Radial Power Profile

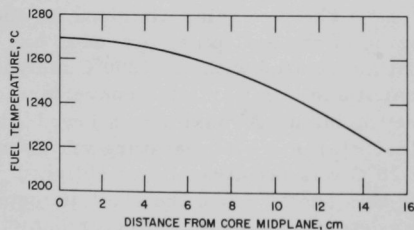
The governing criterion for the sizing of the heat pipes proved to be that associated with the 1200°C molybdenum shell on which the converters are mounted. A maximum allowed circumferential temperature variation of 20°C was (arbitrarily) established for this shell. Since the shell diameter was determined by the reflector diameter, and the number of heat pipes was established by the number of fuel elements, the thickness and circumferential length



112-8201

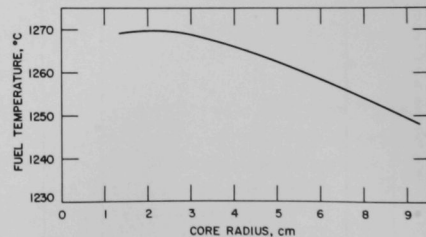
Fig. 8. Fuel-element Peak Temperatures vs Power

verse distribution of heat from the primary pipes and would, moreover, weigh approximately 12 kg less than the solid shell. The wick-pore size for the vapor-chamber web would be identical to that of the primary pipes, since approximately the same wicking height (44 cm) is involved, but the liquid and vapor pressure drops associated with the web would be considerably less, since the distance over which heat is transferred is much smaller (about 0.5 cm).



112-8202

Fig. 9. Core Axial Temperature Distribution



112-8203

Fig. 10. Core Radial Temperature Distribution

The selection of the less elegant, solid shell configuration was, in the end, dictated primarily by considerations of design simplicity.

of the web joining adjacent heat pipes became a function of pipe diameter. On the premise that the inner diameter of the shell was an adiabatic surface, the minimum heat-pipe diameter required to limit the circumferential temperature variation of 20°C was determined to be 1.11 cm (7/16 in.). With this dimension established, the heat pipe easily met the other, and considerably less stringent, requirements. The 1200°C shell configuration selected for the reference design is the simplest, but not necessarily the optimal, design for the hot shell. As shown in Fig. 3, the vapor-chamber web concept could be used to achieve a virtually uniform hot-shell temperature. This involves a somewhat more complex configuration for the hot shell, in that the web structure between the primary heat pipes would contain lithium and would be lined with wicking material similar to that in the primary pipes. This aggregate of vapor-chamber webs would provide nearly isothermal trans-

The theory of heat pipes as presented in Ref. 29 considers solutions of the heat-pipe equations based on the premise that the flow of liquid and vapor in the heat pipe either takes place adiabatically or under conditions of uniform heat input and extraction. In the compact reactor, however, with a "chopped-cosine" axial core-power distribution, this assumption is not valid for the evaporator section of the lithium pipe, although it does apply to the condenser section.

For the in-core heat-pipe design, the liquid and vapor pressure-drop equations were integrated over the evaporator length on the basis of a chopped-cosine power profile using the integrated average radial Reynolds number, a closer approximation to the actual case than is represented by the assumption of a uniform power input. The condenser section was sized on the assumption of uniform power extraction.

C. Heat-pipe Radiator

The radiator (shown in Figs. 1 and 2) consists of an array of 100 rectangular-cross-section heat pipes, which form a cylindrical shell surrounding the electrical generator. The gross dimensions of the radiator were dictated by the 39.5-cm OD assumed for the converter array and by the 510°C cold-junction temperature of the reference thermocouples. For a 4% efficient thermoelectric system, the radiator assembly was sized to reject 26.4 kWt at 500°C with an effective emissivity of 0.85. Its overall length is 113.5 cm. If the reactor were employed with a 1-kWe, 11% efficient thermionic power generator at 600°C collector temperature, the heat-pipe radiator could be dispensed with since direct radiation cooling of the collector would be feasible.

One of the primary advantages of a heat-pipe radiator, which consists of an aggregate of independent cells, is its relative invulnerability to meteor damage. This advantage is partially exploited in the vapor-chamber fin²⁵ Rankine-cycle radiator, but even this advanced-design concept requires some meteor armor to protect the liquid-metal passages from a catastrophic puncture. The concept presented here makes full use of the "independent-cell" feature in that the puncture of any one heat pipe reduces the capacity of the radiator by less than 1%.

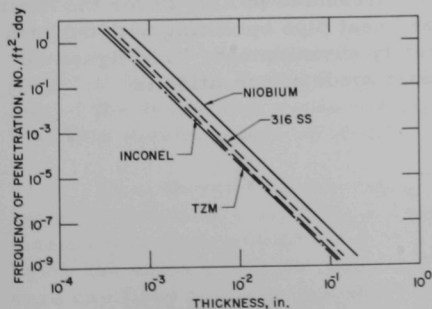


Fig. 11. Frequency of Meteor Penetrations

On the basis of data in Ref. 30, Fig. 11 shows, for several candidate heat-pipe materials, the probable incidence of meteor punctures as a function of armor thickness. The correlation presented by Summers³¹ was used to adapt the data of Ref. 30 to the materials of interest for this study. Figure 11 indicates that the reference

radiator would encounter a meteor sufficiently large to produce a puncture approximately once in 2 years if the heat pipes were constructed of 0.020-in.-thick Inconel tubing. Meteor penetration data are not yet so reliable that information such as that presented in Fig. 11 can be accepted at face value, but since the reference radiator is oversized by 10%, it may be argued that a reasonable rate of attrition of the heat pipes can be tolerated and that no meteor armor is required for this system.

The configuration and operation of the radiator heat pipes is somewhat unusual in several respects: First, the heat pipes are double-ended; that is, heat is added in the central portion of the pipe, and the axial vapor flow is in two directions. Second, the transverse flow of vapor and liquid within the pipe is considerably more complex and less symmetric than for a circular pipe. The vapor produced in the evaporator section on the inner radial surface of the radiator shell condenses on the outer radial surface and flows back to the evaporator via an "upper" and "lower" rectangular wick structure joined by a "lateral" wick (as shown in Fig. 1). A transverse partition, located at the point of zero axial velocity, divides each pipe into two sections, so that the complete radiator shell consists of 200 independent cells.

No satisfactory analytical description of this complicated flow pattern has been developed, nor was its development undertaken for the present study. Rather, the basic heat-pipe theory of Ref. 29 was adapted to the sizing of the wick and vapor passages.

The selection of an optimal fluid for the radiator was less obvious than for the primary heat pipes. Lithium could not be considered, since it is not an effective heat-pipe fluid below 800-900°C because of its low vapor pressure. The choice of fluids therefore lay among the "lower-temperature" liquid metals, such as sodium, potassium, cesium, and rubidium (mercury was ruled out because of its questionable "wetting" properties); the higher-temperature organic materials, such as the family of diphenyls, characterized by Dowtherm; and the molten salts. A figure of merit for heat-pipe fluids can be extracted from the relations presented in Ref. 29 for the limiting heat-transfer capacity of an optimized heat pipe operating with uniform power input and extraction in a zero-gravity environment. This figure of merit for the high radial-Reynolds-number mode of operation is

$$F_H = \mathfrak{L} \left(\frac{\rho_V \rho_\ell \gamma^2}{\mu_\ell} \right)^{1/3},$$

where

\mathfrak{L} = latent heat of vaporization,

ρ_V = vapor density,

ρ_l = liquid density,

μ_l = liquid viscosity,

and

γ = surface tension.

Figure 12 shows this figure of merit as a function of temperature for several of the liquid metals, Dowtherm, and molten sulfur.

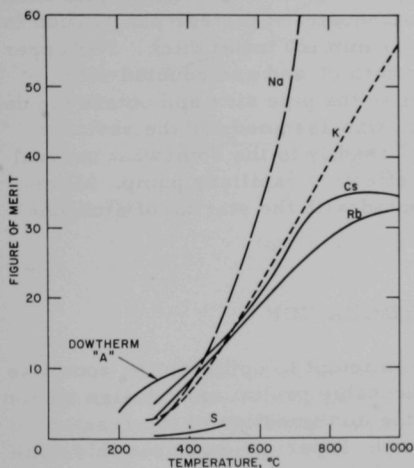


Fig. 12. Figure of Merit for Heat-pipe Fluid

heat-pipe fluid. These conclusions are supported by the results of heat-pipe experiments conducted at LASL with potassium and sodium.

For the primary heat pipes, it was possible to contemplate ground operation of the reactor heat source and high-temperature shell in the "upright" position, because of the excellent wicking properties of lithium. Operating the radiator heat pipes in a vertical orientation, however, it would require a wick-pore structure that could lift the potassium to a height of 56.75 cm (half the length of the radiator) to ensure that the lower half of the evaporator would be wetted. The wick-pore radius associated with this wicking height is about 0.04 mm.

Even though this extremely small pore radius can probably be attained in practice, a large wick cross-sectional area would be required (assuming a wick porosity of 0.5) to maintain the liquid-pressure drop well below the vapor pressure (approximately 0.5 psi at 500°C) and thereby ensure capillary pumping capability and operation in the "heat-pipe regime." This would result in a large pipe with a large cross-sectional aspect ratio.

potassium, rubidium, and cesium appear to be approximately competitive with one another in the temperature range of interest. On the basis of the figure-of-merit curves alone, cesium would appear to be the optimal choice. However, its surface tension is relatively low; hence, its capillary-pump characteristics are not as good as those of potassium. The selection of potassium for the radiator heat-pipe fluid was based on the fact that the performance of this metal has been verified in tests at LASL, and that below about 400°C, the slope of the figure-of-merit curve for potassium is less than that for sodium or the other liquid metals, so that better startup performance at low temperatures can be anticipated. Above 500°C, sodium is clearly superior to the other liquid metals as a

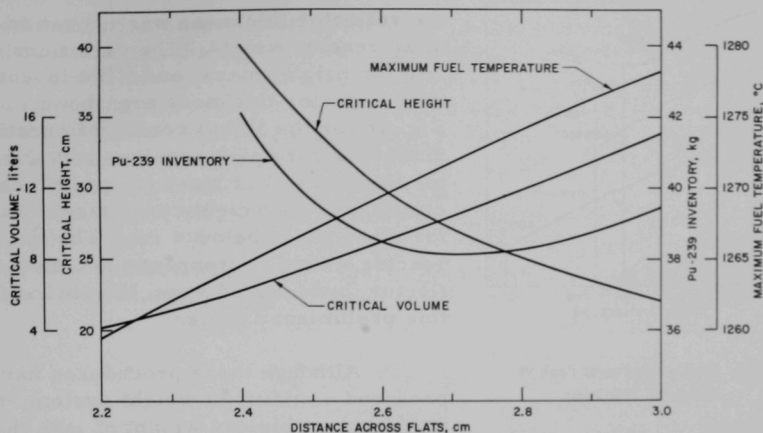
On the premise that the radiator could be ground-tested in a horizontal attitude, the pore radius of 0.025 cm was sized to yield a wicking height of approximately 8 cm. This resulted in a pipe having a 1.34- by 2-cm cross section, so that ample margin is allowed for capillary pumping in a horizontal-attitude ground test of the integrated system.

The heat-pipe wick and tube are fabricated from Inconel. This selection was based primarily on considerations of long-term materials compatibility with potassium, and secondarily on the basis of the fact that Inconel is a reasonably good material from the standpoint of meteor penetration (as shown in Fig. 11). The tube walls are 0.51 mm (20 mils) thick. The upper and lower Inconel wicks are each 0.314 cm thick and are coupled with 0.157-cm-thick lateral wicks. To minimize the pipe size and obtain the desired wicking height, a screen-mesh wick was assumed for the radiator heat pipes. The screen mesh lends itself readily to the somewhat unusual configuration of the wick, and is a more effective capillary pump. Moreover, the vapor-liquid interaction associated with the startup of a channel wick is minimized.

V. REACTOR OPTIMIZATION

Although it would be premature to attempt to optimize the complete system in a study of limited scope, a reasonable preliminary design should consider localized optimization such as the minimization of the reactor weight (core, core container, and reflector). Superimposed upon this consideration are obvious constraints such as those associated with material temperature limits and the attainment of such desirable features as power flattening, the ability to increase the design power level, and various aesthetic aspects of a good design.

If the 7/16-in. OD of the lithium heat pipes is regarded as a fixed core parameter, then one of the important variables that control core criticality is the thickness of fuel surrounding each pipe. This is quantitatively represented by the distance across flats (DAF) of the hexagonal PuP fuel element. Figure 13 shows the variation of fuel loading, core height, and maximum fuel temperature with fuel-element size for a 5-cm BeO reflector. Since the required fuel loading is approximately constant for $2.6 \text{ cm} \leq \text{DAF} \leq 2.8 \text{ cm}$, the lower end of this range was chosen for the preliminary design since it results in a lower fuel temperature, a lower heat-pipe surface heat flux, and correspondingly greater potential for power uprating.



112-8204

Fig. 13. Core Parameters vs Fuel-element Size

VI. RADIAL REFLECTOR

A radial reflector of beryllium oxide is incorporated in the reactor design to minimize fuel loading and total mass, flatten the power distribution, and provide shielding for the thermoelectric version of the system. Radial power flattening is of importance, since it equalizes the thermal

load on the heat pipes and thereby ensures a more uniform temperature along the circumference of the hot shell. With regard to the shielding capacity of the reflector, the dose rate at the reflector outer surface is not necessarily reduced by the reflector since the core power density increases in inverse proportion to the core volume change associated with the reflector savings (as may be seen in Fig. 14). Although power peaking can occur near the outer edge of the core, this problem is avoided if the reflector is less than 8 cm thick (as shown in Fig. 15).

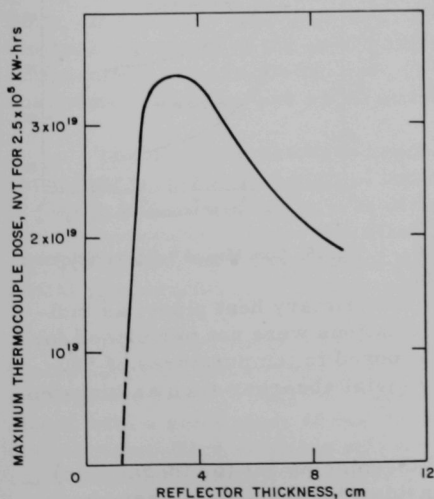


Fig. 14. Dose Rate vs Reflector Thickness

Within the constraints imposed by the requirements for neutron shielding and the necessity of power flattening without flux peaking,

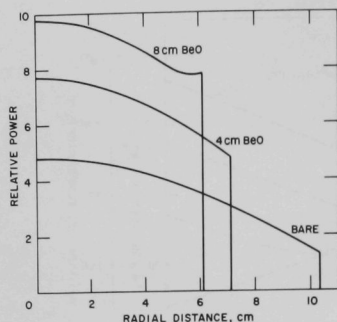


Fig. 15. Core-edge Power Peak vs Reflector Thickness

525 lb with a 4% efficient, 1-kWe thermoelectric generator is indicative of the performance potential of this concept. An obvious improvement would result from a combined core (DAF), reflector, and primary-heat-pipe optimization. Furthermore, design changes such as the use of smaller heat pipes and a modified hot-shell structure would significantly reduce the specific weight, particularly for a high-power (5-kWe) version.

The above comments also apply to a thermionic version of this same system, where the performance improvements associated with optimizing the basic core-reflector-primary-heat-pipe combination would be even more significant.

VII. NUCLEAR SHIELDING

As shown in Fig. 1, provision was made for an uncooled shadow shield between the core and the thermoelement array. This shield would be pierced by the primary heat pipes, as indicated in the figure. Detailed design calculations were not performed for this shield; however, since it would be exposed to temperatures of 500-1200°C, a composite of BeO and a heavy metal absorber such as tungsten would probably be most appropriate.

The possibility of an unshielded thermoelement (or thermionic) array was considered in view of the considerable number of unmanned missions for which a power supply of this kind might be considered.

the reflector thickness was chosen to minimize reactor weight. The variations of reactor height, mass, and ^{239}Pu inventory with reflector thickness are shown in Fig. 16 for the actual core configuration. Since this core plan requires a BeO reflector thickness of at least 1.5 cm to achieve criticality, the weight curve rises sharply for thicknesses below 4 cm. The minimum reactor weight corresponds to a BeO reflector thickness of 5 cm, the choice for this preliminary design.

Although these procedures have not produced a minimum weight system, the predicted unshielded weight of less than

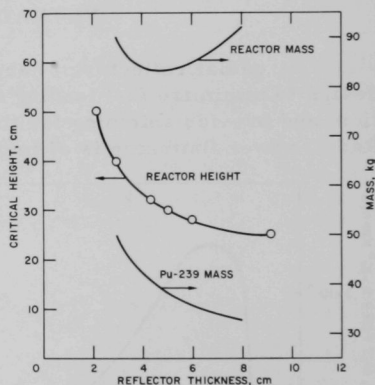


Fig. 16. Core Mass vs Reflector Thickness

The deterioration normally encountered in thermoelectric materials exposed to nuclear radiation could be expected to be minimal for the 1200°C reference thermocouples, since they operate at a temperature in excess of the annealing temperature of the thermoelement material. However, since the reference thermocouples are a boron-based segmented design, there is also a question of deterioration due to an $n-\alpha$ reaction in the boron. The $n-\alpha$ conversion would probably account for less than 0.1% of the thermocouple material during the 10,000-hr mission lifetime; however, since no tests have been performed to verify the radiation tolerance of the reference thermocouples, it is necessary to assume for the purposes of the present study that shielding is required even for unmanned missions.

VIII. CONTROL

The analysis of the control characteristics of a reactor designed for unattended operation may conveniently be divided into two problem areas: (1) control of the large reactivity variations in startup and shutdown, and (2) compensation for the small, gradual reactivity loss due to fuel burnup. Both problems involve the estimation of the temperature and power coefficients of reactivity, since these quantities must be negative to ensure stability and thereby achieve passive control of the system during normal, steady-state operation.

A. Reactivity Coefficients

A temperature increase affects the system geometry in two directions. It produces a prompt axial radial displacement of the fuel due to thermal expansion of the core. None of the other mechanisms for coupling temperature and reactivity, such as Doppler broadening-void formation or spectrum hardening, are applicable to this system.

The axial temperature coefficient ($-6 \times 10^{-6}/^{\circ}\text{C}$) was determined by expanding a 15-cm half-slab of homogenized core material by a factor $(1 + \alpha_{\text{PuP}} \Delta T)$, where α_{PuP} = thermal-expansion coefficient of PuP, and ΔT = fuel-temperature change, and diluting the fuel-number densities by its reciprocal. Thermal expansion of the fuel and the core structure governs the radial temperature coefficient, which was determined to be $-3.5 \times 10^{-5}/^{\circ}\text{C}$.

The radial temperature coefficient was calculated on the basis of the assumption that the array of fuel elements making up the core would undergo the same amount of radial thermal expansion that would be associated with a solid mass of fuel having the same geometry and temperature distribution. This situation will prevail if the fuel elements are mechanically "bundled" so that they remain in contact with one another during the heatup phase and operating life of the core. This can be accomplished if the outer ring of fuel elements is restrained by an arrangement of leaf springs. These springs would be fabricated from tungsten-rhenium alloy,

which can maintain an adequate spring constant at core temperatures. Such springs were proposed for use in the SNAP system.

B. Startup

Control of the reactor over the large reactivity range associated with a transition from cold shutdown to operating power requires a modification of the system geometry. In general, movable absorbing rods or vanes will not provide enough controllable worth, especially when system weight must be minimized.

From the standpoint of weight, reactivity worth, and simplicity, the best startup control scheme involves motion of reflector segments. As derived from Fig. 17, the total worth of the reflector is 22.1% Δk . Although

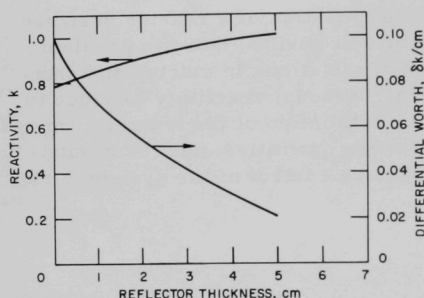


Fig. 17. Reactivity vs Reflector Thickness

the curve of differential reflector worth supports the obvious conclusion that a slab of BeO immediately adjacent to the core is worth more than one at the outer edge of the reflector, practical design considerations require that the control segments include the full reflector thickness (5 cm). Furthermore, the hexagonal nature of the heat-pipe array and the location of the internal structural supports favor a 60° span for these segments.

The reactivity decrement from criticality at zero power to full power can be estimated by multiplying the temperature coefficient ($4.1 \times 10^{-5}/^{\circ}\text{C}$) by the rise from the ambient (30°C) to the nominal operating temperature (1220°C). Assuming that a shutdown margin of 6% Δk is adequate, the required reactivity control is 11.1% Δk , which corresponds to three full-length (30-cm), 60° reflector segments.

The system is started up by slowly inserting two of the three 60° reflector segments, each of which is connected to a small stepping motor (2°/step) through a screw drive (10 pitch). When fully inserted, these two pieces bring the reactor critical at an equilibrium temperature of about 300°C. At this temperature, lithium is still frozen in the heat pipes; heat transfer from the core is by pure conduction; and the reactor power is therefore very low. The third 60° segment is then inserted under the feedback control of a temperature sensor to bring the reactor up to its nominal operating temperature of 1200°C.

The entire startup program occurs slowly enough to permit uniform heatup of the system, which passes through a series of quasi-equilibrium criticality-temperature states during the start sequence.

The desired heatup rate is easily attained by presetting the frequency of the pulses that activate the stepping motors.

With the system stabilized at its operating temperature and power level, the startup controller is permanently deactivated, and the steady-state operating condition is maintained by means of totally passive temperature-coefficient control.

For the reference design, the burnup of 13.2 g of ^{239}Pu or 2.19 cc of the homogenized core material corresponds to 2.5×10^5 kW-hr. This burnup, less than 0.05%, will have no effect on fuel properties. The reactivity decrement corresponding to this fuel loss is $2.67 \times 10^{-4} \Delta k$. This can be compensated for by a drop in the core temperature of 6.5°C . Fuel temperature permitting, if the maximum allowable ΔT during a 10^4 -hr mission life were -50°C , the maximum reactor power could be 192 kWt.

IX. CONCLUSIONS

The power-supply concept presented in this report is the result of a mating of three compatible products of current technology: (1) the compact, high-power-density fast reactor, (2) an advanced high-temperature fuels technology, and (3) the liquid-metal heat pipe. The reactor system described here was configured as a space power supply on the basis of projected space power requirements of the 1979's, since it appears to fill a need for a reliable, uncomplicated, high-temperature heat source that can match recent advances in thermoelectric and thermionic converter technology.

Since the 1-kWe system described here was configured as an all-purpose, 1-10-kWe generator, with growth potential as a major design goal, it can hardly be regarded as optimal for a given power level or mission. Rather, it was intended to serve as a vehicle to explore the feasibility of a concept through the medium of a point design. The optimization of the system for a given power level, mission, or type of converter would involve some changes of the reference design. For example, undersea and terrestrial versions of the system would be tailored to other means of heat rejection than thermal radiation.

We believe that this passively controlled, compact, fast-reactor concept, combined with the unique advantages of a heat-pipe power transfer and heat-rejection scheme, represents an interesting challenge to isotopes in the low-to-medium power range where they have thus far enjoyed virtually uncontested supremacy.

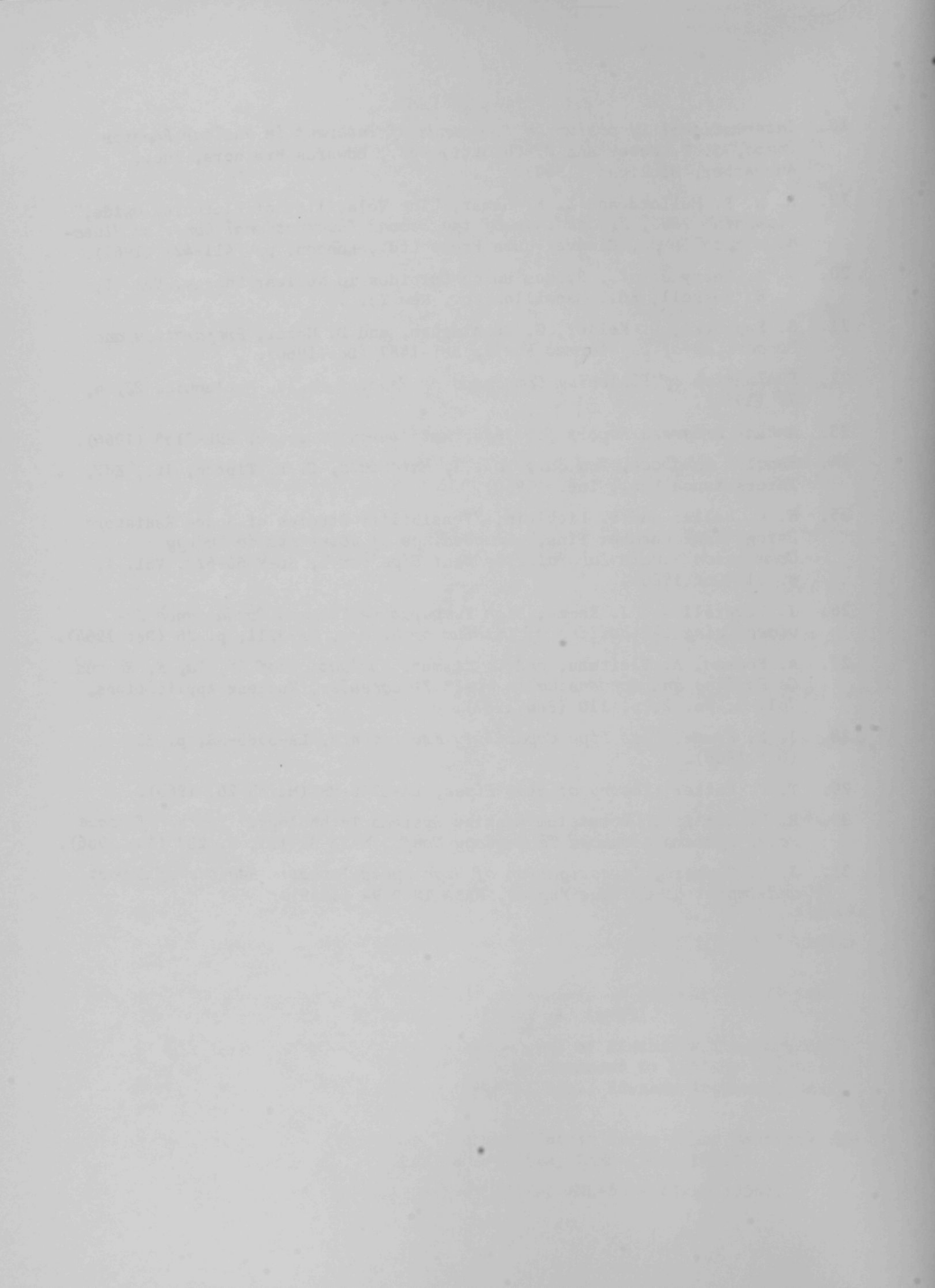
ACKNOWLEDGMENT

We are indebted to Dr. Owen L. Kruger of Argonne National Laboratory, who provided expert advice on reactor-fuels technology.

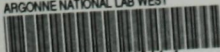
REFERENCES

1. J. D. Gylfe and R. E. Wimmer, "Reactor-Thermoelectric Power Systems for Unmanned Satellite Application," *Trans. Intersociety Energy Conversion Engineering Conf.*, Los Angeles, Calif., pp. 84-93 (Sept 1966).
2. E. D. Harris and D. J. Dreyfuss, "Manned Spacecraft Electrical Power Systems: Requirement Weight Correlation and Cost Implications," *Trans. Intersociety Energy Conversion Engineering Conf.*, Los Angeles, Calif., pp. 162-171 (Sept 1966).
3. *High Temperature Thermoelectric Research*, AFAPL-TR-64-135, Air Force Aero Propulsion Laboratory, Wright-Patterson Air Force Base, Ohio (Dec 1964).
4. J. C. Danko, G. R. Kelp, and P. V. Mitchell, "Irradiation Effects on Thermoelectric Materials," *Advanced Energy Conversion*, Vol. 2, Pergamon Press, pp. 79-85 (1962).
5. G. N. Hatsopoulos, "Thermionic Energy Conversion," *Trans. Intersociety Energy Conversion Engineering Conf.*, Los Angeles, Calif., pp. 238-244 (Sept 1966).
6. W. B. Hall et al., *Development of a Low Temperature Cylindrical Thermionic Generator*, APL-TR-65-41 (April 1965).
7. W. B. Hall and S. W. Kessler, *Development of a Flame Fired Thermionic Generator*, AD 634-538 (April 1966).
8. W. E. Harbaugh, *Development of an Insulated Thermionic Converter Heat Pipe Assembly*, AFAPL-TR-66-37 (May 1966).
9. D. R. MacFarlane, *A 200-watt Conduction-cooled Reactor Power Supply for Space Application*, ANL-6694 (March 1963).
10. Milton Shaw, "AEC Programs and Requirements for Plutonium," CONF-660308, *Commercial Plutonium Fuels Conf.*, Washington, D.C., pp. 6-13 (March 1966).
11. Glenn T. Seaborg, "Plutonium - Past, Present, Future," CONF-660308, *Commercial Plutonium Fuels Conf.*, Washington, D.C., pp. 60-68 (March 1966).
12. O. L. Kruger and J. B. Moser, *Preparation of the Sulphides and Phosphides of Plutonium*, *J. Inorganic Nuclear Chemistry* 28, 825-832 (1966).
13. O. L. Kruger, private communication to J. J. Roberts, Argonne National Laboratory (Jan 1966).
14. O. L. Kruger, *Preparation and Some Properties of Arc-Cast Plutonium Monocarbide*, *J. Nuclear Materials* 7, 2, 142 (1962).
15. O. L. Kruger, "Constitution and Properties of Plutonium Monocarbide," *International Symposium on Compounds of Interest in Nuclear Reactor Technology*, J. T. Weber and P. Chiotti, Eds., Edwards Brothers, Inc., Ann Arbor, Michigan (1964).
16. G. E. Hansen and W. H. Roach, *Six and Sixteen Group Cross Sections for Fast and Intermediate Critical Assemblies*, LAMS-2543 (1961).
17. J. R. Novak, Ed., *Radiation Safety Guide*, ANL-5574 (June 1956).

18. *International Symposium on Compounds of Interest in Nuclear Reactor Tests*, J. T. Weber and P. Chiotti, Eds., Edwards Brothers, Inc., Ann Arbor, Michigan (1964).
19. R. N. R. Mulford and L. E. Lamar, "The Volatility of Plutonium Oxide," *Plutonium 1960, Proceedings of the Second International Conf. on Plutonium Metallurgy*, Cleaver-Hume Press Ltd., London, pp. 411-421 (1961).
20. J. A. Leary *et al.*, *Symposium on Carbides in Nuclear Energy*, Vol. I, L. E. Russell, Ed., Macmillan Co., New York.
21. S. Paprocki, D. Keller, G. Cunningham, and D. Kozier, *Preparation and Properties of UO₂ Cermet Fuels*, BMI-1487 (Dec 1960).
22. *Evaluation of Plutonium Compounds as Reactor Fuels*, *Nucleonics* 23, 4, 72 (1965).
23. *Annual Progress Report for 1965*, *Metallurgy Division*, ANL-7155 (1966).
24. *Reactor Handbook*, 2nd Ed., Vol. I, *Materials*, C. R. Tipton, Jr., Ed., Interscience Pub., Inc. (1960).
25. H. C. Haller and S. Lieblein, "Feasibility Studies of Space Radiators Using Vapor Chamber Fins," *Proceedings of Joint Atomic Energy Commission/Sandia Laboratories Heat Pipe Conf.*, SC-M-66-623, Vol. 1, p. 51 (Oct 1966).
26. J. Deverell and J. Kemme, *High Temperature Thermal Conductance Devices Using the Boiling of Lithium or Silver*, LA-3211, p. 26 (Oct 1964).
27. A. Romano, A. Fleitman, and C. Klamut, *Evaluation of Li, Na, K, Rb and Cs Boiling and Condensing in Nb-1% Zr Capsules*, *Nuclear Applications*, Vol. 3, No. 2, p. 110 (Feb 1967).
28. J. E. Kemme, *Heat Pipe Capability Experiments*, LA-3585-MS, p. 33 (Oct 1966).
29. T. P. Cotter, *Theory of Heat Pipes*, LA-3246-MS (March 26, 1965).
30. R. E. English, "Potassium Rankine Systems Technology," *Trans. of Space Power Systems Advanced Technology Conf.*, NASA SP-131, p. 237 (Aug 1966).
31. J. L. Summers, *Investigation of High Speed Impact: Regions of Impact and Impact at Oblique Angles*, NASA TN D-94 (1959).



ARGONNE NATIONAL LAB WEST



3 4444 00011244 1

X